Indian Journal of Engineering & Materials Sciences
Vol. 30, June 2023, pp. 396-401
DOI: 10.56042/ijems.v30i3.3669

Thickness dependent structural, optical, and electrical properties of ZnSe thin films

Tripti Gupta* & R P Chauhan
Department of Physics, National Institute of Technology, Kurukshetra, Haryana 136 119 India

Received: 10 May 2023; Accepted: 30 May 2023

In present work, nanostructured films of ZnSe are synthesized on glass substrates by using electron beam vacuum evaporation technique. To enhance the luminescence performance and electrical conductivity, the optimal film thickness are investigated for which films of thickness 250 nm and 500 nm are grown on glass substrates. Additionally, films' crystal structures are also characterized. The XRD pattern revealed that the synthesized films exhibit preferred orientation of ZnSe (111) lattice which exhibits polycrystalline state having cubic zinc blende structure. Various structural parameters such as their crystallite sizes, strain developed in films, and their dislocation densities are also calculated. UV/VIS/NIR spectrophotometer indicates that visible transmittance decreased while the infrared transmittance switching efficiency increased as the film thickness increased from 250 nm to 500 nm. Moreover, the optical energy gaps of ZnSe films were in a range of 2.1-2.20 eV which is comparatively smaller in comparison to their bulk counterparts revealing their confinement in nano-dimensions. The study of their luminescence properties yields that the film of thickness 250 nm yield better results in blue spectral region which is also illustrated through CIE plots. The reason could be that for smaller film thickness electrons can easily jump to excited states for similar excitations owning to smaller crystallite sizes and thus showed greater luminescence. However, from the analysis of its electrical characteristics, the enhanced electrical conductivity is captured for the films having thickness of 500 nm. Therefore, the enhanced blue emission in the optimized film thickness indicates that these films can be utilized as luminescent materials.

Keywords: ZnSe, Thin Films, Transmittance Spectra, Photoluminescence, Electrical Properties

1 Introduction

Thin films of II-VI group compound semiconductors have not only established their tremendous utility in numerous electronic applications at the commercial levels for many years, but also played a significant role in the evolution of semiconducting device physics. From various II-VI group compounds thin films of Zinc Selenide (ZnSe) is a compound of prominent interest because of its countless applications in optoelectronic devices. This compound possess a direct bandgap of 2.7 eV and is transparent over wide range of visible spectra. Infact, it is the most used material in infrared applications due to its low dispersion rate and high refractive index. It has also popularly been used for fabricating red, blue, and green LEDs[1-3] due to its wide range of transmission, thin film transistors[4], photovoltaics[5-7], photoelectrochemical cells[8,9] etc. Due to its low electrical resistivity, direct bandgap, high luminescence, high optical transmission, and good photosensitivity it can be used as a window layer in solar cells[10,11]. Moreover, it can be used as a substitute in replacing toxic Cadmium Sulphide, as ZnSe is environmentally safe and fits better in solar spectrum. Various techniques have been used for the growth of high-quality ZnSe thin films such as sputtering technique, electrochemical deposition, thermal evaporation, chemical bath deposition[12-17].

Among numerous techniques used for the deposition of ZnSe thin films, electron beam evaporation is the most attractive one due to fabrication of very high purity thin films as in this synthesis takes place under strong vacuum environment. It is well known that the optical properties and structural characteristics of films rely mostly on environmental parameters in which the process of deposition is being performed. Additionally, in this technique the rate of deposition is comparatively high and during the course of deposition the damage introduced to the substrate can also be reduced. Many parameters for the synthesis of ZnSe thin films have been optimized which have already been reported in literature. But study on variation in thickness of thin films using electron beam evaporation are still scare which brings out the significance of present undertaken work.

*Corresponding author (E-mail: triptigupta2211@gmail.com)

Recently, optical thin films have developed keen interest due to their wide range of applications in the field of optics, electronics, and photonics. In order to have applications of thin films, coatings are required to have improved optical properties, like higher transmission efficiencies, lower residual loss because of reflection, and wide bandwidth. For such types of films, their characteristic sizes are known to be as small as that of nanoscale levels. The properties and structures of nanodimensional films are quite distinct in comparison to those of their bulk counterparts. Analysis of their electrical properties also plays a significant role to have their applications at the industrial levels in fabricating nano-electronic circuits, window layers of solar cells etc.

Here, in the undertaken work ZnSe thin films have been fabricated on the glass substrates at the thickness of 250 nm and 500 nm using electron beam evaporation synthesis method. The influence of film's thickness on optical, structural, and electrical characteristics are scrutinized and studied in detail.

2 Materials and Methods

2.1 Fabrication of ZnSe thin films

Pure ZnSe powder having 99% purity purchased from Sigma Aldrich was employed for the fabrication of thin films. Firstly, ZnSe pallet of 10 mm diameter was made by applying the pressure of 4-5 tonns through (KBr Press, Model M-15) a hydraulic pressure machine. Then glass substrates were cut into small square pieces of area 1 cm^2 and were thoroughly cleaned in ultra-sonicator to remove all the stagnant dirt and contamination deposited over them. For which, initially they were cleaned using detergent for approx. 15 min, followed by sterilizing them in deionized water (DI), then in acetone, and lastly in isopropyl alcohol, respectively. Then these cleaned glass slides were dried in an electric oven. Thereafter, thin films having thickness of 250 nm and 500 nm were deposited onto substrates of glass at room temperature using TVE (Vacuum Box Coater HHV BC-300) deposition technique employing the optimized controlled parameters. Sample holder was loaded with ZnSe pallet in the tungsten spring holder and was situated at 15 cm of distance away from source and was continually rotated to have uniform deposition over the glass substrate. The thickness of film and its evaporation rate were monitored using Quartz microbalance (Model DTM-101, HINDHIVAC) which is inbuilt in coating machine. Penning and pirani gauges were utilized to maintain (1- 2) × 10^{-5} mbar of pressure. As soon as substrate temperature reaches value of melting point target i.e., ZnSe, current of 10-12 ampere begins to flow through pallet which deposits ZnSe in the form of thin films at the glass substrates. The rate of evaporation at the time of deposition was 4-5Å/sec.

2.2 Characterizations

The crystalline structures and phase identification of ZnSe thin films were carried out using X-Ray Bruker D8 Advance Diffractometer having radiations of Cu-k_α of 1.54 Å wavelength in 2θ range of 20°- 90°. Debye-Scherrer method was utilized for estiating their crystallite sizes. To study the optical characteristics of fabricated thin films of ZnSe, the optical transmittance spectrum was studied through Shimadzu UV-VIS-NIR Spectrophotometer UV-3600 Plus and optical emission spectra was obtained using SHIMADZU RF-530 spectrophotometer at room temperature with an excitation using Xe lamp at wavelength of 350 nm. 2-probe method of Ecopia Probe station along with Keithley 2400 series source meter was employed to investigate the electrical properties of deposited thin films at thickness of 250 nm and 500 nm.

3 Results and Discussion

3.1 Structural Analysis

XRD analyses of the as-synthesized thin films were carried out to examine their structural characteristics. ZnSe thin films developed at 250 nm, and 500 nm thickness on substrates of glass are depicted in Fig. 1.

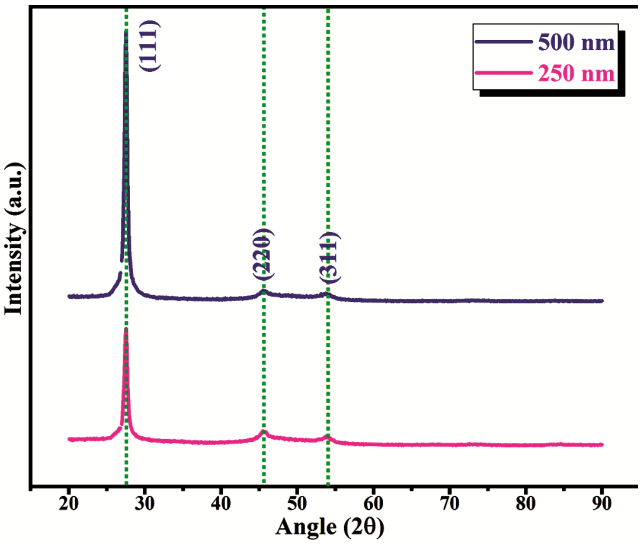

Fig. 1 — XRD patterns of thin films at thickness of 250 nm and 500 nm.

The XRD patterns of thin films at 250 nm and 500 nm thickness exhibits three diffraction peaks of (111), (220), and (311) ZnSe planes at 2θ values of 27.5°, 46.6°, 53.0°. XRD pattern comprises of crystal planes which belongs to distinct families is an indicative of film's polycrystalline nature. For both the films, (111) peak is the prominent peak. Although, with increase in films thickness, intensity of XRD peak increased sharply and the peak become more narrow. This is due to the reason that with increase in path length of X-rays in the film of higher thickness, more number of atoms will contribute towards X-ray diffraction hence grater intensity or higher height of diffraction peak is obtained. This is the reason behind variation in intensity with film thickness. It indicates that with increase in the thickness of films, the crystalline quality of films gets improved. However intensity of other two peaks almost remained the same. The intensity of peaks and their crystallite sizes are related to film's crystallinity. In 250 nm thin films incomplete crystallites growth leads to poor crystallinity[18]. According to mechanism of growth[19,20], developing faces of crystallites corresponds to shape of crystal. In accordance to orientation, a growth competition begin among neighboring crystals. The free surface is formed once competition go ahead towards the formation of crystal faces of similar type. This mode of competitive growth is a depictive of selection of orientation[21]. This probably be the reason for improvement in thin films crystallinity with increased thickness. The intensity of peaks represents preferable Miller planes orientation of films[22]. Hence, texture coefficients of both films are calculated in order to quantify preferred orientation of planes using Eq. 1[23].

$$TC = \frac{I(hkl)/I_0(hkl)}{\frac{1}{n}\sum I(hkl)/I_O(hkl)} \quad \ldots (1)$$

Here, I(hkl) represents measured peak' relative intensity of (hkl) plane, I_o (hkl) represents standard relative intensity of plane, and n denotes the peak number.

From Table 1, the preferred crystallographic oriented plane is the one whose TC value exceeds 1. For both the films grown at 250 nm and 500 nm thickness, the preferred crystallographic plane is (111), since the TC value for this plane only exceeds unity. Various structural parameters such as crystallite sizes (average), dislocation densities, and their microstrain are also calculated and mentioned in Table 2. Debye Scherrer equation was used to calculate crystallite size (average)[22].

$$D = k\lambda/\beta Cos\theta \quad \ldots (2)$$

Here, k is crystal shape constant having value of 0.9, λ is the wavelength of X-ray, β is FWHM (Full Width at Half Maxima), D is crystallite size, and θ indicates diffraction angle. The microstrain is calculated using [24]:

$$\varepsilon = \frac{\beta}{4\,tan\theta} \quad \ldots (3)$$

and the Dislocation density was also calculated through the equation[25]:

$$\delta = \frac{1}{D^2} \quad \ldots (4)$$

Table 2 clearly indicates that with variation in the thickness of thin films, their structural parameters also gets influenced. In case of 250 nm thick films, the value of strain produced is high thus leading to comparatively smaller crystallite size. The fraction of energy deposited while fabricating the films of higher thickness leads towards variation in the orientation of granules due to alteration in the positioning and

Table 1 — Texture coefficient (TC) values for thin films at 250 nm and 500 nm thickness

Planes	Texture Coefficient	
	250 nm	500 nm
(111)	2.66	2.87
(220)	0.18	0.06
(311)	0.14	0.14

Table 2 — Structural parameters of thin films deposited at 250 nm and 500 nm thickness

Thin Films (Thickness)	2θ (degree)	Miller Indices (hkl)	FWHM (degree)	Average crystallite size	Strain ($\times 10^{-3}$)	Dislocation density ($\times 10^{15}$ m^{-2})
250 nm	27.51498	(111)	0.6282	5.72 nm	30.95	30.56
	46.13657	(220)	4.64623			
	52.98352	(311)	3.89026			
500 nm	27.51533	(111)	0.54528	6.58 nm	29.13	23.07
	46.64037	(220)	5.20595			
	53.35244	(311)	2.87674			

boundaries of grains. Therefore, smaller grains aggregated to form grains of comparatively larger sizes, possessing lesser values of strains and dislocation densities.

3.2 Optical Analysis

3.2.1 UV-Visible Spectroscopy

Optical properties of thin films of ZnSe were studied by obtaining transmittance spectra in the spectral range from 100 nm to 1000 nm measured with the help of UV-Vis spectrophotometer as shown in Fig. 2. Low transmittance is observed for wavelengths below 400 nm and transmittance was seen to increase with increasing wavelength. Thus, it can be inferred that ZnSe in thin film form has good transmittance for higher wavelengths. Also the sensitivity of 250 nm ZnSe thin film was found to be higher than 500 nm thin films. The thin film with lesser thickness showed low transmission at lower wavelength lower than the thicker film and showed higher transmission at higher wavelengths higher that thicker one. However, both the films showed excellent transmitivity in blue green region of visible spectrum of light. Films of lesser thickness are more strained, have small size crystallites and weak orientation which leads to high absorbing films. ZnSe has good absorbance for blue light and less absorbance for higher wavelength.

The optical bandgap of the films were also evaluated using Tauc and Menth relation[26]:

$$(\alpha h\nu) = k(h\nu - E_g)^n \quad \ldots (5)$$

Here, hν represents energy of photon, α is coefficient of absorption, E_g represents bandgap and for the direct bandgap transitions the value of exponent n is chosen to be ½. From the above relation we can find the optical band gap (E_g) by extrapolating the (αhν)^2 Vs eV curve on to horizontal axes. In this experiment, the optical energy gap of thin films of ZnSe were obtained to be 2.05 eV and 1.91 eV for 250 nm and 500 nm thickness films respectively. The existence of disorders causes creation of energy level in the forbidden gap which ultimately results to diminished energy gaps. Some of the probable reasons behind decrease in bandgaps with increase in the thickness of films are:

(a) As the thickness of film increases, the localized states within the forbidden gap gets enhanced contributing towards smaller bandgaps.
(b) With increase in film thickness, The Fermi level approaches the top of valence band causing decline in the forbidden energy bandgap.
(c) As the film thickness is increased, the light beam transmittance usually gets declined and gets shifted towards higher wavelengths, causing shifting in the optical absorption edges towards higher wavelengths i.e., lower photon energy, leading towards decrease in optical bandgap.
(d) With increase in thickness of films, there is decrease in the angle of refraction of incident light beam within thin film materials, leading towards an increment in the refractive index of films hence, the bandgap gets reduced.

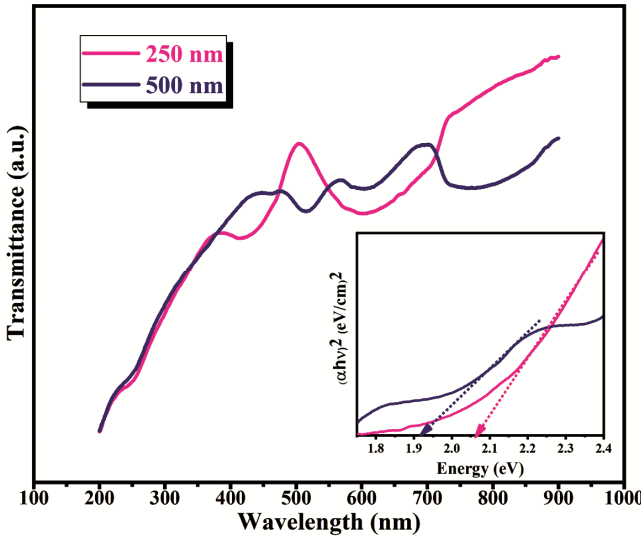

Fig. 2 — Transmittance spectra and inset is Tauc plot of ZnSe thin films having thickness 250 nm and 500 nm.

These band gap is lower to theoretical value of 2.7 eV owing to quantization effect occurring due to thin film nature of subject material. ZnSe in amorphous state has a large band gap however in thin film form ZnSe particles were less strained than that in powder form. Thus, ZnSe thin films have slightly more conductive nature than its powder form and hence lower optical band gap.

3.2.2 Photoluminescence Spectroscopy (PL)

The luminescence property of ZnSe thin film grown onto glass substrates was studied by analysis the emission spectra. In this experiment, ZnSe thin films of 250 nm and 500 nm were excited using Xenon light source at room temperature.

As indicated in Fig. 3, the emission spectra of photoluminescence for both the samples exhibit four main emission bands. Two strong emission bands were obtained near 430–440 nm and 460–470 nm whereas two weak bands around 415 and 500 nm. First band represents the UV emission peak near 415 nm (3.0 eV).

The second peak is due to intrinsic intra-band gap defects which occured because of both ZnO and ZnSe. Due to this defect the donor levels are created near the band edge of conduction band. The third recorded strong emission peak lies in the blue region of visible spectra which corresponds to near band - edge excitons emission, because the energy gap of pure ZnSe material at room temperature is about 2.7 eV (460 nm). The last peak around 500 nm is the weakest emission peak which is because of existence of non-stochiometric point defects. Therefore, both samples exhibits typical luminescence behaviour having dominant emission intensity peak around 460 nm. From Fig. 3, a typical decline in peak intensity is observed with increase in film thickness due to strong dependence on surface area of grains. It is crucial to control surface states in order to have well defined excitonic emission or bandgap. Usually, with increase in grain sizes, the surface state density decreases. In addition, the intensity of luminescence also decreases with depreciation in the surface states density owing to comparatively smaller surface to volume ratios for the crystallites of larger sizes. Hence, films having larger crystallites exhibits lower intensity of luminescence in comparison to those having smaller crystallite sizes.

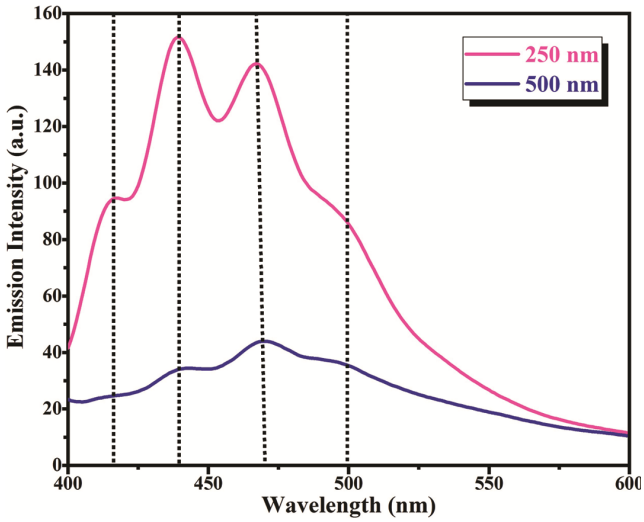

Fig. 3 — Photoluminescence spectra of thin films at thickness of 250 nm and 500 nm.

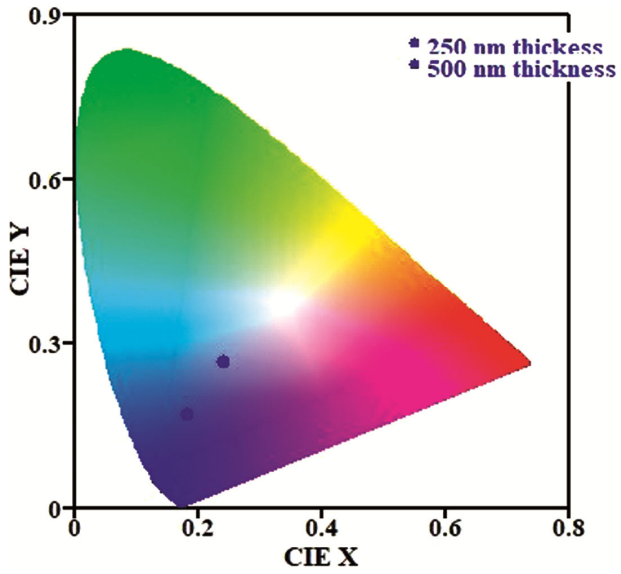

Fig. 4 — CIE (Commission Internationale de l'Éclairage) 1931 color diagram of 250 nm and 500 nm ZnSe thin films.

Figure 4 illustrates the chromaticity coordinates in CIE 1931 plots for the 250 nm and 500 nm ZnSe thin films. The coordinates obtained for 250 nm ZnSe thin films are (X: 0.18; Y: 0.17), whereas for the 500 nm ZnSe thin films are (X: 0.24; Y: 0.27). Both of these lies in the blue region of visible spectra indicating that ZnSe thin films can be used in fabricating blue LEDs.

3.3 Electrical Analysis

To have the utilization of ZnSe thin films at practical level in designing of solar cells, the study of its electrical characteristics becomes significant. In the present study, equally spaced ohmic type contacts are designed on the thin films through paste of silver and the paint brush. For measuring their electrical conductivity a Keithley source meter and a two probe set-up was used in -10 to +10 V of voltage range. The current voltage properties of 250 nm and 500 nm films are illustrated in Fig. 5.

For both the thickness a symmetrical curves are obtained in the I-quadrant and III-quadrant indicating the synthesized films are of ohmic nature, thus making

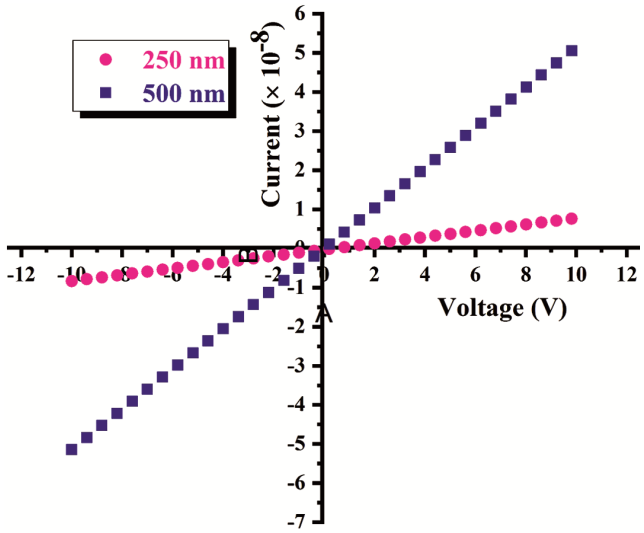

Fig. 5 — I-V characteristics of thin films at thickness of 250 nm and 500 nm.

them a suitable contender for the fabrication of optoelectronic devices. The obtained curves were fitted linearly. The I-V characteristics of films thus obtained shows a greater slope for thin film with 500 nm than 250 nm. Since the bandgap of 500 nm thin films were smaller in comparison to 250 nm films hence providing greater amount of conductivity due to low hindrance for electrons to jump from valence to conduction band. It could be inferred that 500 nm film showed greater degree of conductivity.

4 Conclusion

The current research work aimed at scrutinizing structural, luminescent, and electrical characteristics of thin films of ZnSe grown at the thickness of 250 nm and 500 nm. At first we obtained zinc selenide thin films over substrate of glass by Electron-beam vacuum evaporation synthesis method for two different thicknesses of 250 nm and 500 nm respectively. Structural characteristics was obtained by doing XRD analysis of the thin films. Structural analysis showed increased in peak intensity with increased in the thickness of films revealing that (111) plane of ZnSe is the dominant crystal plane for both the deposited films. It could be inferred that thin films of 250 nm thickness were more strained than the 500 nm, thus the crystallite size of 250 nm thin film were smaller compared to 500 nm. UV-Vis spectroscopy and PL spectroscopy of thin films revealed their optical characteristics. Optical transmittance spectra studies revealed, ZnSe has high transmittance and luminescence for the films with lower thickness. The corresponding Tauc plots indicated decline in the bandgap with increase in Film's thickness. From Photoluminescence spectra along with their CIE plots manifests that these thin films can be suitable for the designing blue LEDs. For studying conductivity of the films, current-voltage characteristics was obtained in the region -10V to +10V. Film with greater thickness was found to be more conductive in nature and represented an increasement in the mobility of charge carriers and their concentration with increase in the thickness of film from 250 nm to 500 nm. The reported results in present work are advantageous in optoelectronic devices designing, fabrications of optical coatings for IR applications and developing the solar cell's window layer.

Acknowledgment

Authors are thankful to the Director, National Institute of Technology Kurukshetra for providing the research facilities. The authors yearn to acknowledge the Director (MNIT Jaipur) for providing High Vacuum Thermal e-beam coating unit (Model BC-300 HHV) for obtaining ZnSe thin film on glass substrates. Authors also express their gratitude to Dr Sanjeev Aggarwal, Director of Ion Beam Center, Kurukshetra University, Kurukshetra for allowing the requisite facilities of characterization crucial to effectively execute the present study.

References

1 Güzeldir B, Sağlam M, & Ateş A, *J Alloys Compd*, 506 (2010) 388.
2 Othonos A, Lioudakis E, Tsokkou D, Philipose U, & Ruda HE, *J Alloys Compd* (2009) 483 (2009) 600.
3 Ippen C, Greco T, Kim Y, Kim J, Oh MS, Han CJ, & Wedel A, *Org Electron*, 15(2014) 126.
4 Alfano RR, Wang QZ, Jimbo T, Ho PP, Bhargava RN, & Fitzpatrick BJ, *Phys Rev A*, 35(1987) 459.
5 Toma O, Ion L, Iftimie S, Antohe VA, Radu A, Raduta AM, & Antohe S, *Appl Surf Sci* 478 (2019) 831.
6 Bang J, Park J, Lee JH, Won N, Nam J, Lim J, & Kim S, *Chem Mater*, 22(2010) 233.
7 Toma O, Antohe VA, Panaitescu AM, Iftimie S, Răduţă AM, Radu A, & Antohe Ş, *Nanomaterials*, 11(2021) 2841.
8 Lohar GM, Jadhav ST, Takale MV, Patil RA, Ma YR, Rath MC, & Fulari VJ*, J Colloid Interface Sci*, 458 (2015) 136.
9 Lohar GM, Dhaygude HD, Patil RA, Ma YR, & Fulari VJ, *J Mater Sci Mater Electron*, 26(2015) 8904.
10 Abdalameer NK, Mazhir SN, & Aadim KA, *Energy Rep*, 6 (2020) 447.
11 Chuhadiya S, Sharma R, Patel SL, Chander S, Kannan MD, & Dhaka MS, *Phys E Low-Dimens Syst Nanostructures*, 117(2020) 113845.
12 Khan TM, Mehmood MF, Mahmood A, Shah A, Raza Q, Iqbal A, & Aziz U, *Thin Solid Films*, 519(2011) 5971.
13 Mahalingam T, Dhanasekaran V, Chandramohan R, & Rhee JK, *J Mater Sci*, 47(2012), 1950.
14 Bakiyaraj G, & Dhanasekaran R, *Appl Nanosci*, 3(2013) 125.
15 Khalfi R, Talantikite-Touati D, *Tounsi A, & Merzouk H, Opt Mater*, 106 (2020) 109989.
16 Li S, Wang L, Su X, Pan Y, Gao D, & Han X, *Thin Solid Films*, 692 (2019) 137599.
17 Ke J, Zhang R, Zhang P, Yu R, Cao X, Kuang P, & Wang B, *Superlattices Microstruct*, 156 (2021) 106965.
18 Seto JY, *J Appl Phys*, 46(1975) 5247.
19 Van der Drift A, *Philips Res Rep*, 22(1967) 267.
20 Knuyt G, Quaeyhaegens C, D'haen J, & Stals LM, *Phys Status Solidi B*, 195(1996) 179.
21 Barna PB, & Adamik MJTSF, *Thin solid films*, 317(1998) 27.
22 Cullity BD*, Addison-Wesley Publishing*, (1956).
23 Harris GB, *The London, Edinburgh, and Dublin Philosophical Magazine and Journal of Science*, 43(1952) 113.
24 Williamson GK, & Smallman RE, *Philosophical magazine*, 1(1956) 34.
25 Stokes AR, & Wilson AJC, *Proceedings of the Physical Society* (1926-1948), 56(1944) 174.
26 Tauc J, & Menth A*, J Non Cryst Solids*, 8 (1972) 569.